Gaseous Micropattern Detectors: High-Energy Physics and Beyond

Archana Sharma[1]
University of Maryland, College Park, 20742 MD, USA

Abstract

Multiwire gaseous detectors have matured in the last few decades with major implications in particle physics experiments. They have also been successfully refined for use in other fields: X-rays for medical imaging, UV and single photon detection, neutron and crystal diffraction studies, etc. Their major limitation has been a modest rate capability (10^3/mm^2). In the last decade, several micropattern position sensitive gas devices have been introduced with an inherently improved rate capability (few MHz/mm^2) and a localization accuracy of 40-50 µm. They are being extensively pursued for their application in several fields. The state-of-the-art of this new generation of gaseous detectors will be reviewed.

INTRODUCTION

The pioneering work done at the beginning of the twentieth century by Thomson, Rutherford, and Geiger [1] just after the discovery of electromagnetic radiation, focussed attention to the development of tools to detect radiation. The Single Wire Proportional Counter (SWPC) was one of the essential tools in the early part of the last century.

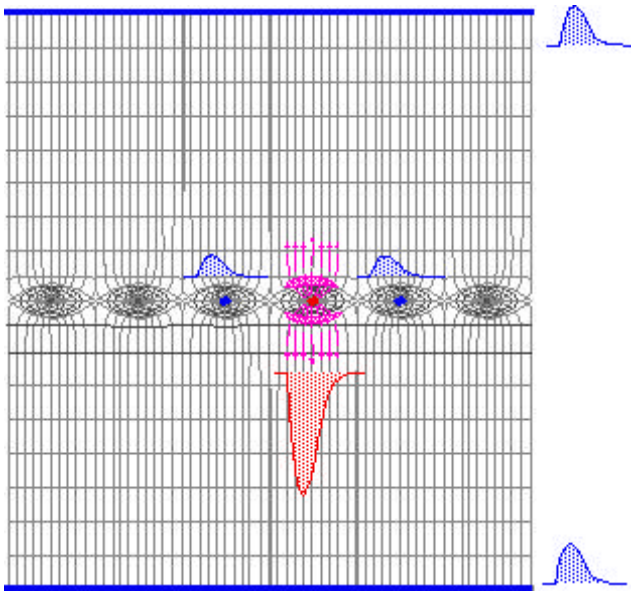

Fig. 1. Principle of the Multi-Wire Proportional Chamber (MWPC).

[1] Presently at CERN, CH 1211, Geneva, Switzerland. E-mail: Archana.Sharma@cern.ch

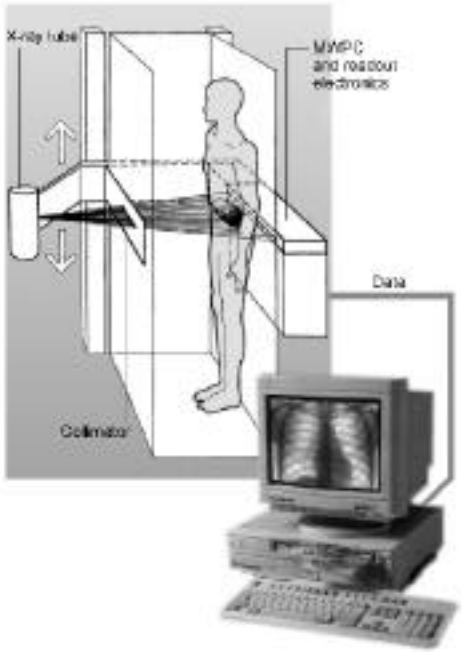

Fig. 2. The Siberian digital radiography device using MWPC [4].

It was not until the invention by Charpak in 1968 of the Multi-Wire Proportional Chamber (MWPC), see fig. 1 and Ref. 2, that a new era was ushered in this field. The main performance features of the MWPC are a space resolution of few hundred μm, two- and three-dimensional localization of incident radiation, excellent energy resolution, rate capabilities of a few kHz/mm^2. Two track separations of the order of 2 mm have been measured and very large active areas and volumes have been effected over the last three decades for charged particle tracking in medium and high-energy physics. Several excellent review articles have been written on the subject; a selection is given in Ref. [3].

Some applications of MWPCs may be cited as crystal diffraction, beta chromatography, and dual energy angiography. A low dose X-ray digital radiography scanner based on the MWPC (see Fig. 2) was invented by the BINP Novosibirsk group [4], and is presently being applied routinely to examine patients in hospitals in Russia and in France [5,6]. Fig. 3 taken from [6] shows a film of a congenital hip dislocation (Perthes disease) in a 7-year-old boy with satisfactory visualization of the femoral architecture and bone texture. Upgrades of this device for improved resolution and dose reduction are still in progress [6,7].

Fig. 3. Digital Radiography of a child with congenital hip dislocation using MWPC Scanner.

Despite their success, some fundamental limitations of multiwire proportional chambers restrict their use for high-rate application. Detailed discussions of these characteristics may be found in the cited literature: the wire spacing limits the position accuracy and two-track resolution to ~ 1mm. The electrostatic instability limits the wire lengths. The widths of the induced signal define the pad response function, and most importantly at high rates, accumulation of positive ions restrict the rate capabilities of MWPCs as shown in fig. 4.

The advent of high luminosity colliders [8] demands fast, highly performing position sensitive detectors. Ever more stringent, unsurpassed position, two-track, two-dimensional and time resolutions, ability to operate withstanding long-term radiation and background environment are key requirements.

A concept worth mentioning here is that employed by the Multi-Step Chamber, which was introduced by Charpak and Sauli [3]. It comprises dividing the total gain of the MWPC into two smaller sub critical parts by first allowing the electrons produced by ionizing particles to multiply in the pre-amplification region and then proceed to the anode for further amplification, In this way, the chamber operation was found to be more stable and provided higher gain, as shown in fig 5.

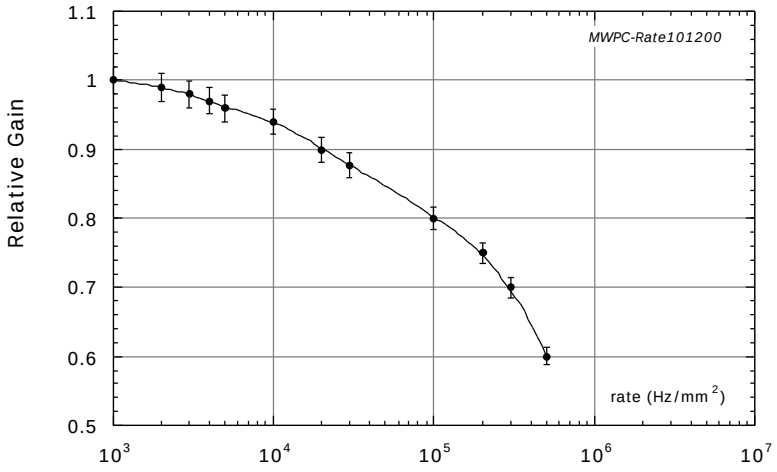

Fig. 4. Rate capability of a Multiwire Proportional Chamber.

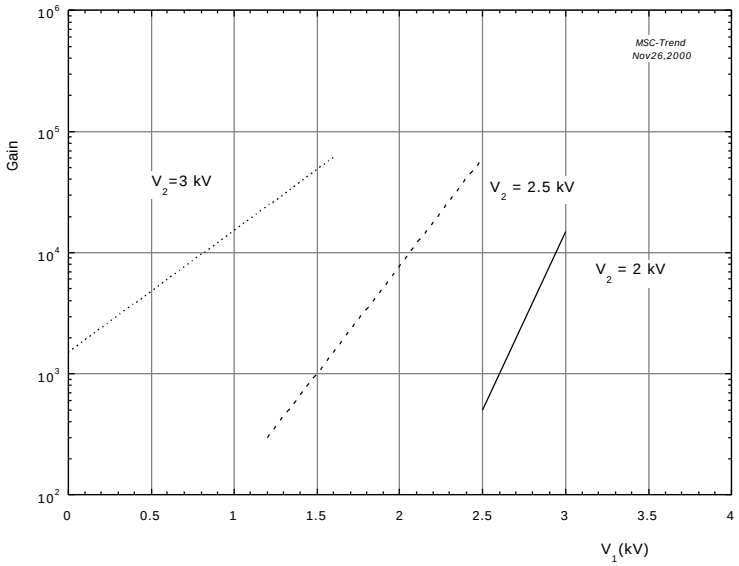

Fig. 5. High gain in a Multi-Step Chamber.

The invention of the Micro-Strip Gas Chamber (MSGC) by Oed [9] ushered another new era of gaseous detectors. A recent review [10] summarizes in detail the MSGCs and its derivatives, here I will briefly mention their key features and some applications.

A. THE MICRO STRIP GENERATION

An MSGC consists of a pattern of thin anodes and cathode strips laid on an insulating substrate with a pitch of a few hundred μm as sketched in fig. 6(a). Delimited by a drift electrode above and appropriate potentials applied, the resulting electric field[2] is as shown in Fig. 6(b). The design itself removes the positive ions from the vicinity of the avalanches, thereby lending high rate capability to this device almost two orders of magnitude higher (~ 10^6/mm^{2}s) than MWPCs (~10^3/mm^{2}s).

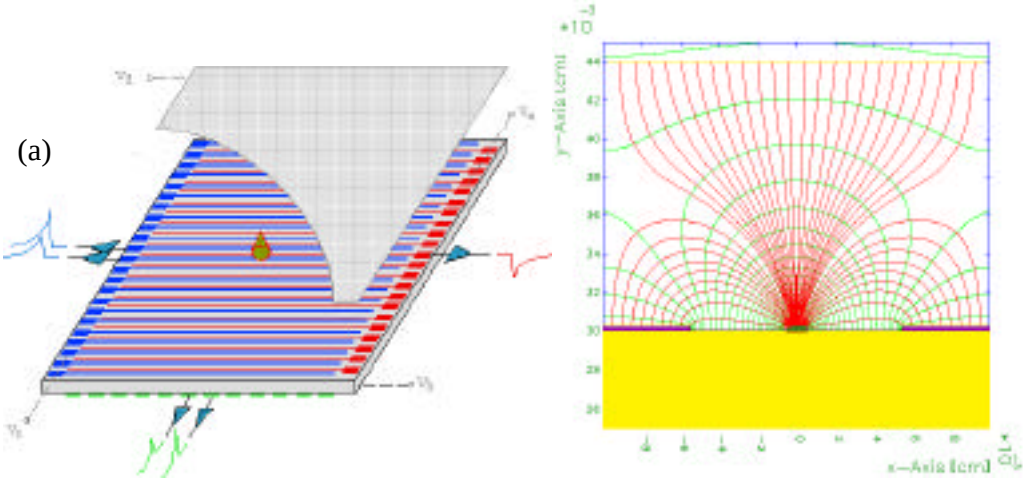

Fig. 6. (a) Principle and (b) Field configuration in an MSGC with typical voltage settings.

The salient features of its operation are localization accuracies ~ 30 μm rms, double track resolution of 400 μm, and good energy resolution. Long-term and magnetic field operations have been demonstrated, and apart from high-energy physics [11], these devices have found application in many varied fields of X-ray spectrometry and digital radiography.

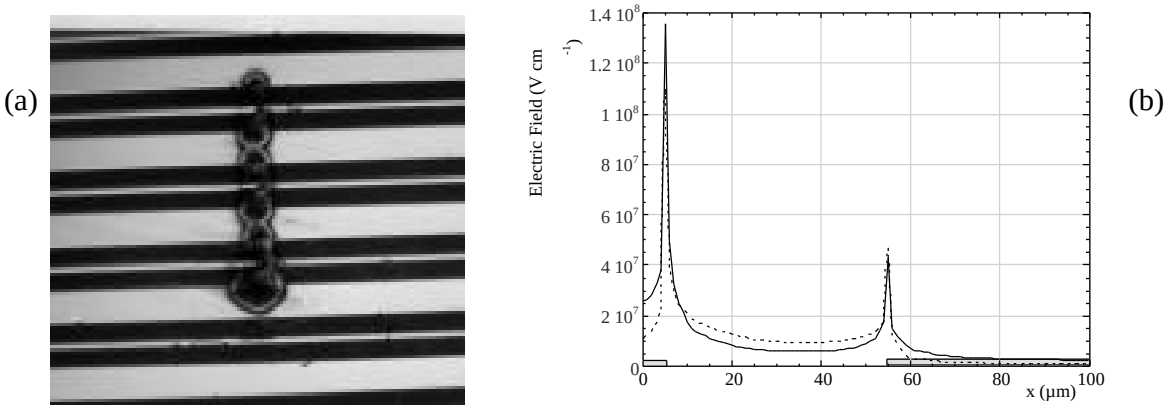

Fig. 7. (a) Damage in an MSGC and (b) Field along the surface of an MSGC.

[2] All electric fields and simulations presented in this work are taken from Ref. 10 or are unpublished work of the author.

The difficulties associated with operating MSGCs [12] began when they were exposed to highly ionizing particles, usually present in a high luminosity machine backgrounds from low energy γ's, proton conversions, and nuclear fragments. The highly ionizing particles deposit almost three orders of magnitude more charge in the detection volume as compared to a minimum ionizing particle. In such a circumstance the avalanche to streamer, and avalanche to gliding discharge, transitions are more likely damaging the strips (see fig. 7a). Several groups dedicated themselves to examine and understand these defects [13-17]. What emerges is that the streamer mode of operation in the case of an MWPC is stable due to the fact that the electric field, shown in fig. 7(b), in the direction of the propagation of the streamer is increasingly weak (between the anode and cathode). In the case of micro-strip detectors, the anode-cathode distance is very small (~50-100 μm). The electric field at the tip of the streamer and that along the surface being high, the streamer is most likely to be followed by a voltage and ionization density dependent discharge. Charging up of surface defects, long-lived excited states, and overlapping avalanches seem to be the culprit lowering the discharge limits of operation of these devices. With this insight, several novel designs appeared on the horizon, some of which are discussed below.

III. THE 'NEW MICROPATTERN' ERA

B. MICRO-DOT AND MICRO-MEGAS

Early attempts to create the first micro-needle structure were done by Spindt et al. as early as 1976. Spindt used them successfully to emit electrons towards the phosphor screen in high vacuum, for the purpose of creation of the flat TV screens. Soon, several people [18], for example Va'vra and later on Oed with his own design of the micro-needle array, have tried to use them as the electron amplifiers in the gas.

(a)

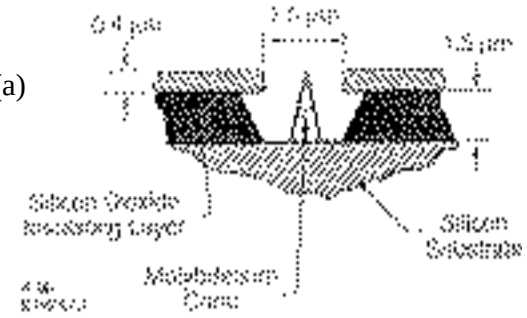

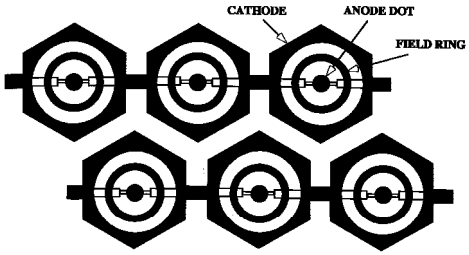

(b)

Fig. 8. (a) The micro-needle structure produced by Spindt et al., (b) Schematic of a Microdot Chamber.

However, no observable gas gain was measured at normal pressure due to the extremely fine needles [<<1μm radius and ~1.2 μm high; see fig. 8(a)], and resulting in very small amplification region. Advances in photolithography and application of silicon foundry techniques heralded a new era in the design and fabrication of "Micropattern Detectors". The Microdot detector (μDOT), sketched in fig. 8, and operated successfully by Biagi [19], is the ultimate gaseous pixel device with anode dots surrounded by cathode rings. The chamber could reach very high gas gains of ~10^6 without a discharge [20].

(a)

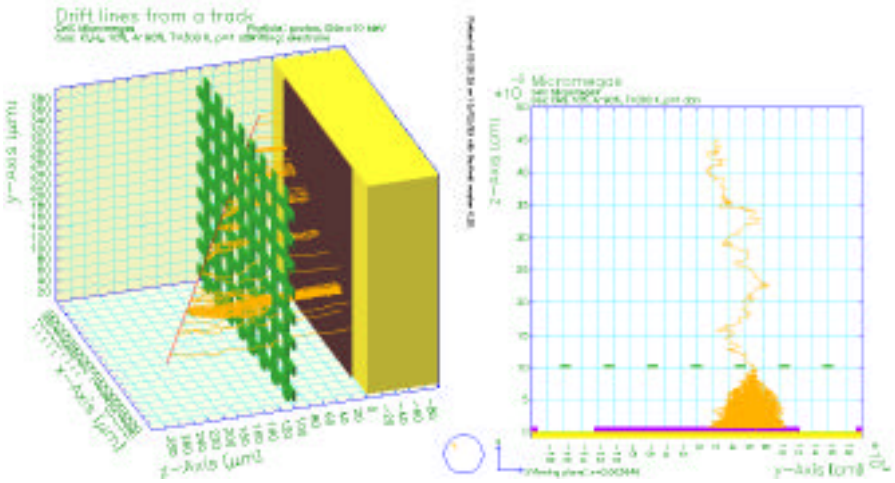

(b)

Fig. 9. (a) Electrons drifting from the sensitive volume into the amplification volume of a MICROMEGAS, (b) An avalanche in a MICROMEGAS detector.

A very asymmetric parallel plate chamber, the MICROMEGAS detector invented by Charpak and Giomataris [21], takes advantage of the semi-saturation of the Townsend coefficient at high fields ~ 100 kV/cm in several gas mixtures [22], thus being stable in its operation with minimum ionizing particles. Fig. 9 shows electrons drifting from the sensitive volume into the amplification volume and an avalanche in the thin multiplying gap. Figure 10 shows the excellent energy resolution of this device. Large area, 40 x 40 cm^2 MICROMEGAS detectors are being made and tested [23] for the COMPASS experiment at CERN; see fig. 11.

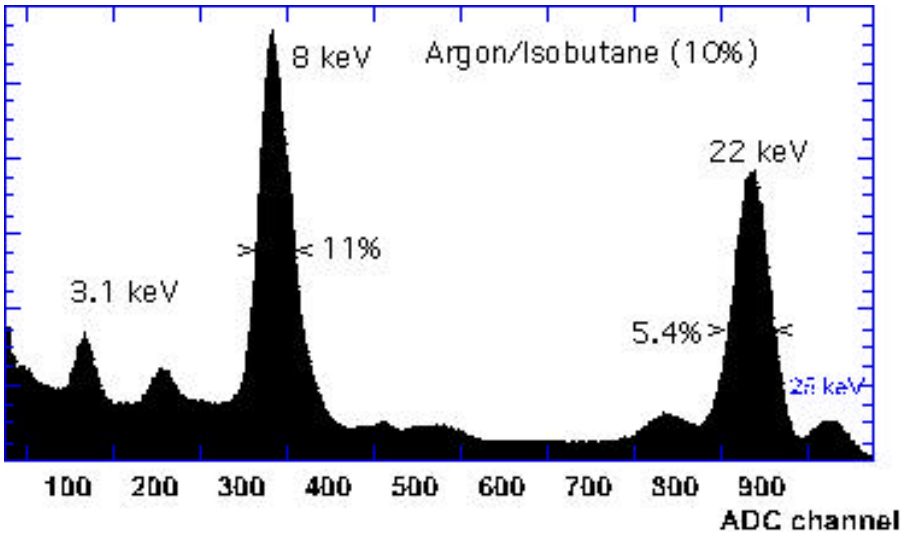

Fig.10. Energy resolution with a MiCROMEGAS detector.

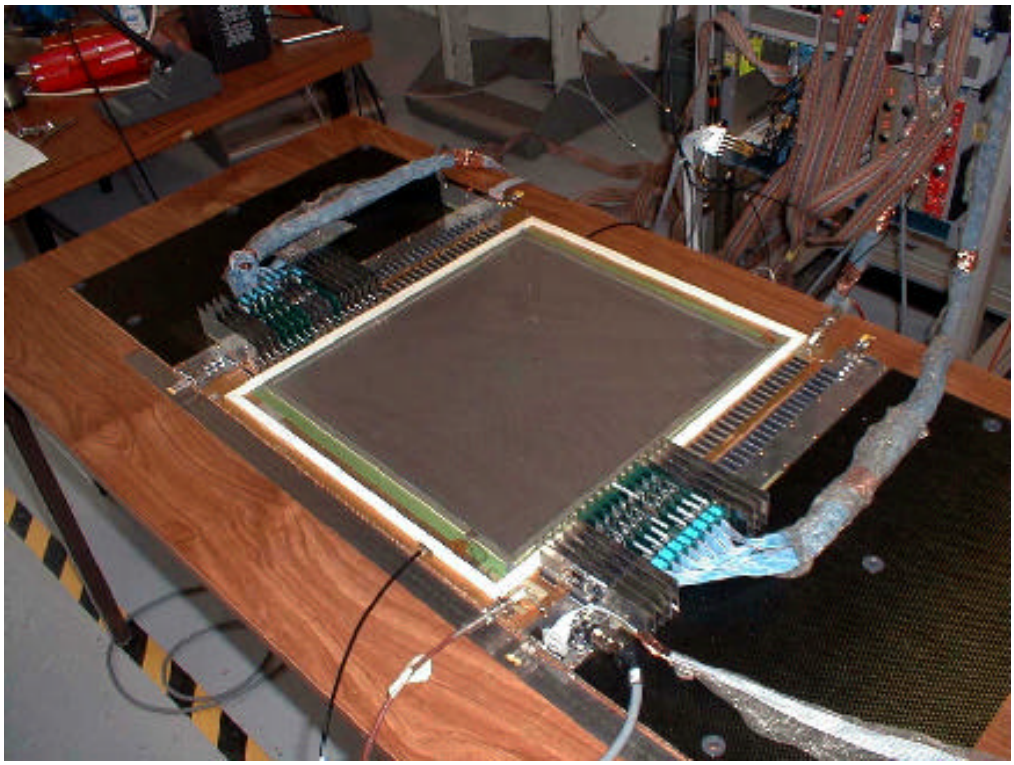

Fig. 11. Large size COMPASS MICROMEGAS prototype.

B. CAT detectors

A new kind of detector was invented by Lemonnier et al. during the same era as the detectors discussed so far, called the CAT or "Compteur A Trous"[3] [24]. It consists of a narrow hole micro-machined in an insulator metallized on the surface as the cathode.

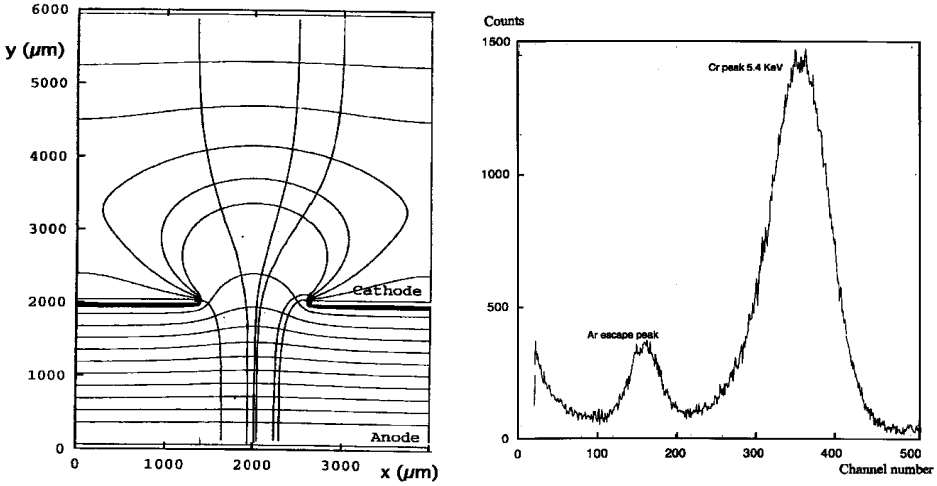

Fig. 12 (a) Electric Field in a CAT, (b) energy resolutio

[3] Patent No. 2727525 dated 25.11.94

The metal at the bottom of the hole constitutes the anode. With appropriate potentials and a drift electrode, this scheme acts as a focussing lens for the drifting electrons left in the wake of ionizing radiation as shown in fig. 12(a). Figure 12(b) shows the typical energy resolution measured with this kind of a device. Removing the insulator in between leaves the cathode as a micro-mesh, which when placed with a thin gap above the readout electrode, emulates the CAT operation hence named micro-CAT or µCAT, see Fig. 13 (a)[25]. This structure could reach gas gain of several 10^4. With an ingenious scheme of readout from virtual pixels made by current sharing, offering 20 times finer resolution as compared to the readout cell (Fig. 13(b)), the µCAT combined with the Virtual pixels is renamed the VIP [26].

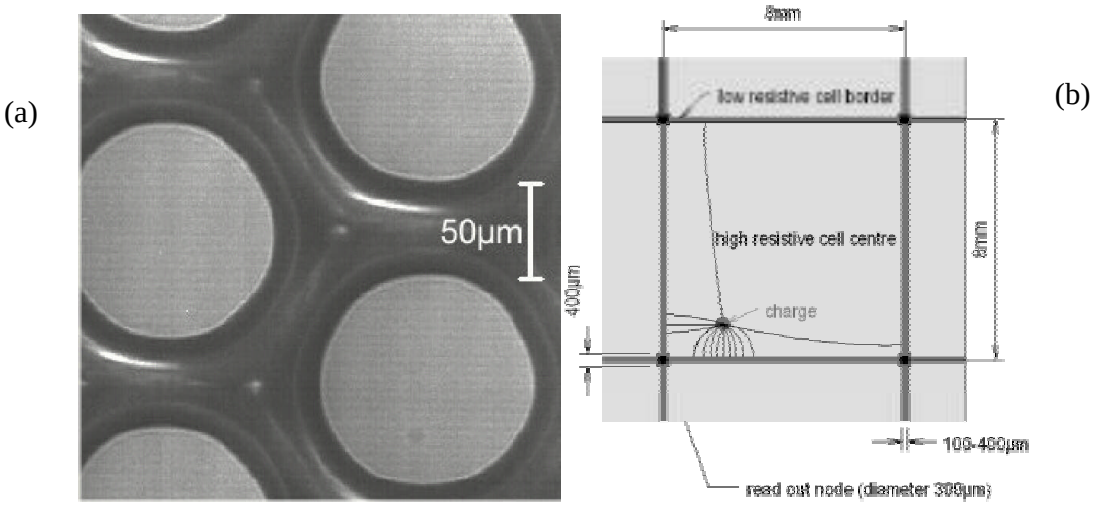

Fig. 13. (a) Microphotograph of a CAT mesh, (b) Virtual Pixel readout scheme.

C. GEM detectors

A new concept of gas amplification was introduced in 1996 by Sauli, the Gas Electron Multiplier (GEM) [27] manufactured by using standard printed circuit wet-etching techniques[4] schematically shown in Fig. 14(a). Comprising a thin (~50 µm) Kapton foil, double-sided clad with Copper, holes are perforated through (Fig. 15b).

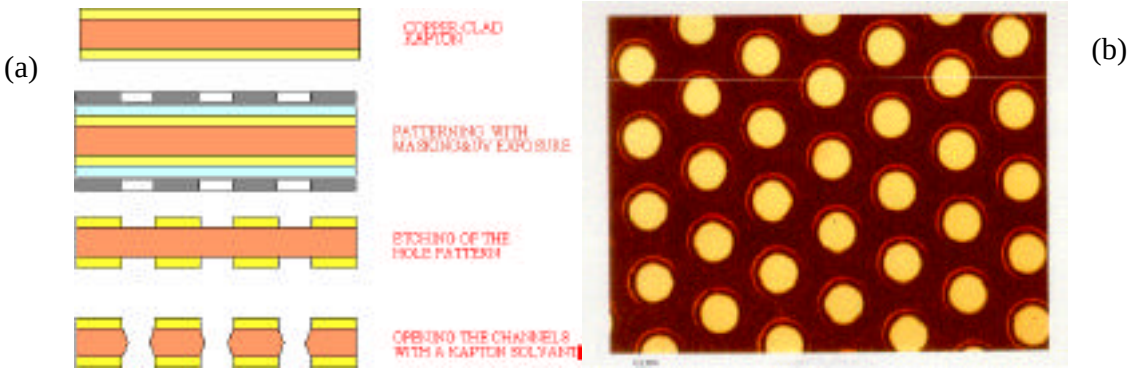

Fig. 14 (a) Chemical etching process of a GEM and (b) A GEM foil

The two surfaces are maintained at a potential gradient, thus providing the necessary field for electron amplification, as shown in Fig. 15(a), and an avalanche of electrons as in Fig. 15(b).

[4] At the Printed Circuit & Surface Treatment Workshop at CERN, Geneva, Switzerland.

(a)

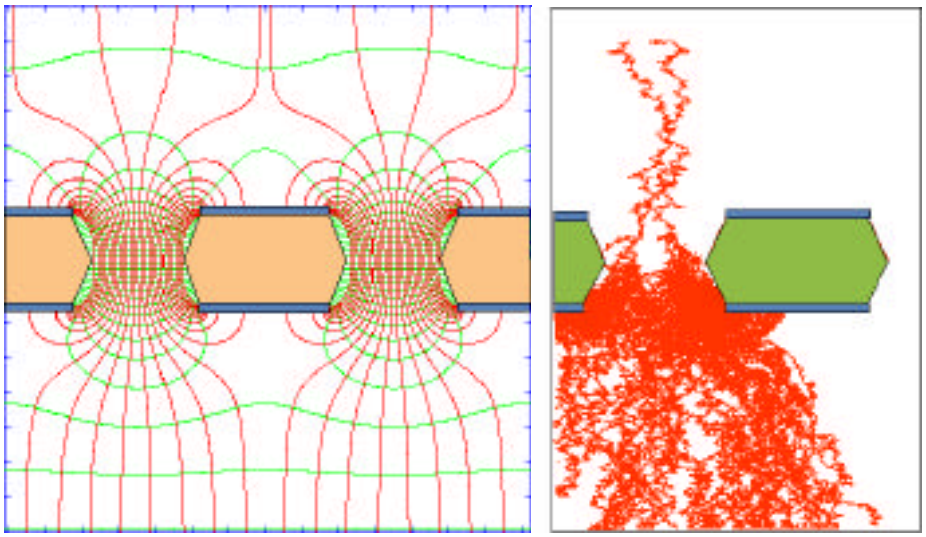

(b)

Fig. 15(a) Electric field and (b) Avalanches across a GEM channel.

Coupled with a drift electrode above and a readout electrode below, it acts as a highly performing micropattern detector. The essential and advantageous feature of this detector is that amplification and detection are decoupled, and the readout board is at zero potential. Permitting charge transfer to a second amplification device, this opens up the possibility of using a GEM in tandem with an MSGC or a second GEM.

D. Other MICROPATTERNS detectors

Following the GEM concept and better understanding of the discharge phenomena, several new 'micro'-detectors have appeared on the scene: Micro-Wire [28], an extension of the µDOT in the third dimension, Micro-Pin Array (MIPA) [29] (see figs. 16a and b), the Micro-Tube [30], Micro-Well [31], Micro-Trench [32] and Micro-Groove [33].

(a)

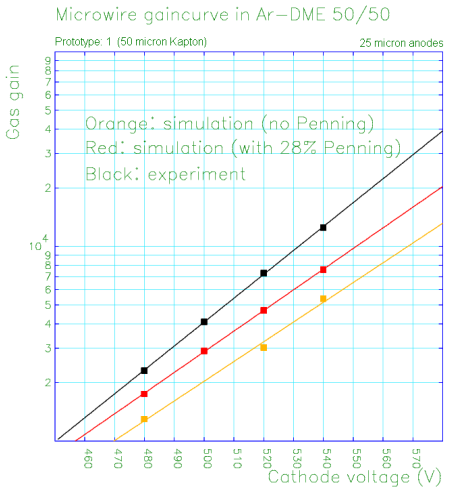

(b)

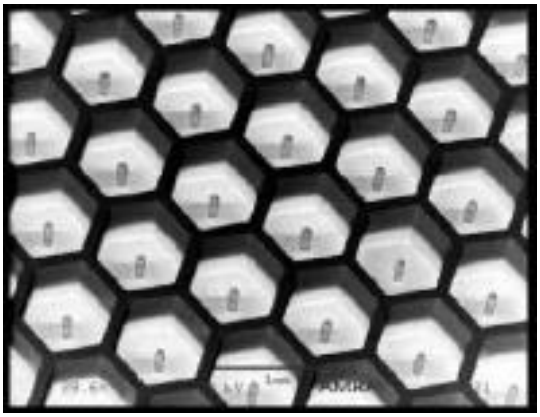

Fig. 16. (a) Gain with a Micro-Wire Detector (b) The MIPA Array.

All these authors have tried to minimize the presence of insulators in between the anode and cathode, which is the culprit for gliding discharges along the surface. Figure 17(a) shows a microphotograph of the Micro-Tube detector, with a field map in Fig. 17(b) [30]. Fabricated using combination of laser micro-

machining and nickel electroplating, it consists of ~150 µm diameter cathode and an anode tube, which is machined through the well and plated alongside.

(a) 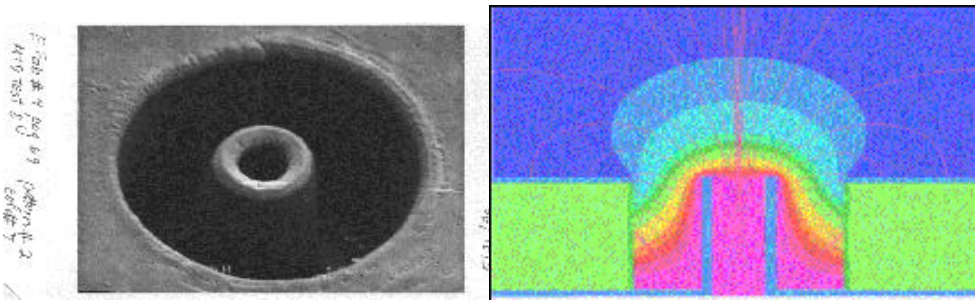 (b)

Fig. 17. (a) The Microtube: the central pin is metallized on the outside, emulating an anode wire, (b) Field across a Microtube.

This structure results in an electric field that increases rapidly at the anode, similar to the µDOT. However, there is no insulating material on the direct line of sight from the cathode to the anode. These design features are predicted to lead to higher gas gains, better stability with fewer discharges, and the reduction of charging effects. An investigation of the effects of detector geometry upon Microtube performance shows similar performance to the µDOT and µCAT detectors, it also predicts large gains ~ 10^4 [30].

As mentioned above, detailed studies have shown that discharges in the presence of highly ionizing particles appear in all micro-pattern detectors at gains of a few thousands [19]. It is possible to obtain higher gains with poorly quenched gases, since they permit a lower operating voltage, and have a higher diffusion, thus lowering the charge density and photon feedback probability. Combining the MSGC with a GEM, safe operation has been demonstrated up to gains of few ten thousands; ~200 of such detectors are operating at HERA-B [34]. The DIRAC [35] experiment at the CERN PS also employs MSGC + GEM detectors, which have permitted to improve the momentum resolution by a factor of two; Fig. 18 (a and b) shows an assembled GEM + MSGC, and is a fine example of vertex reconstruction using this detector.

(a) 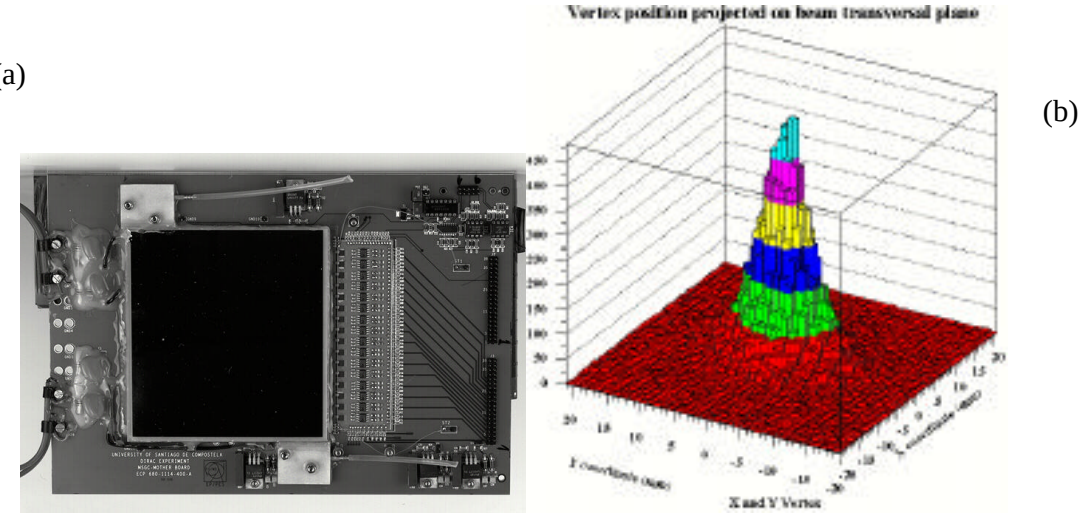 (b)

Fig. 18. (a) An MSGC + GEM assembly for DIRAC tracker, and (b) Vertex reconstruction.

Putting two GEMs in tandem offers a robust detector, which has been studied in detail [36], and large size devices are being built for the COMPASS experiment [37], Carrying the concept further, adding a

third GEM offers an even more stable operation in the worst hadronic beam environment, as demonstrated in Ref. [38]. At gains of ~10^4, spark probabilities (~10^{-10}) have been measured.[5] Figure 19 shows the probabilities of discharges in a single, double and triple GEM detector [37]. For large sizes, the GEMs are segmented in order to reduce the capacity, thus limiting the energy in a discharge.

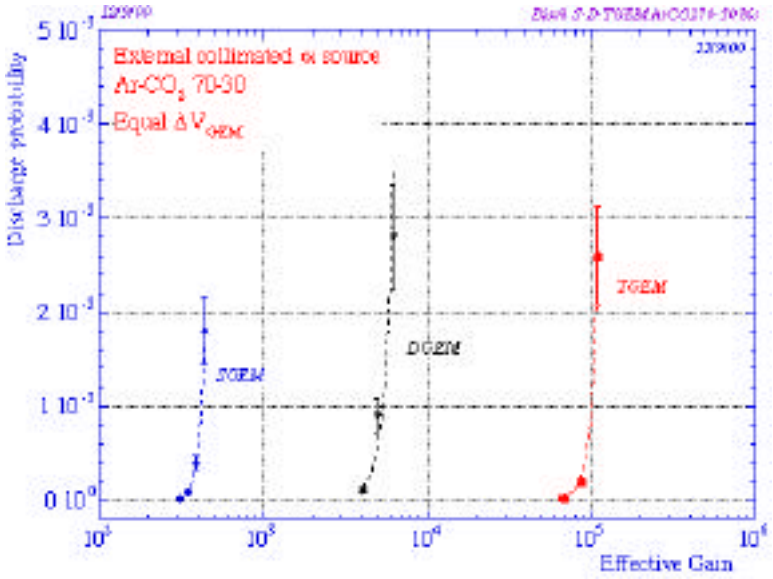

Fig. 19. Probability of a discharge, normalized to the number of heavily ionizing tracks, versus gain for single, double and triple GEM detectors.

IV POTENTIAL APPLICATIONS OF THE "MICRO-GENERATION"

A. MSGCs for X-Ray Imaging

Conventional film radiography has very good spatial resolution, but limited dynamic range. For radiographic film, the storage and display media are the same. For film storage media, dynamic range means that the film image saturates (additional photons do not cause proportional film darkening). The display contrast is fixed at the time of film exposure. One does not see much difference in visible contrast in different parts of a film image, which can have widely different number of photons/pixels. Whereas in a digital system, the storage medium (computer) does not saturate and has infinite dynamic range. The display media being different from storage can be varied at will, i.e., the available display dynamic can be chosen to cover the number N photons/pixel from any N (min) to N(max). The image can be further enhanced using photon energy information. This has been made possible by using the MSGCs with Xe-CH_4 at high pressures; an example of an image is shown in Fig. 20 [39].

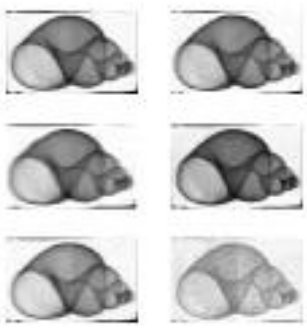

Fig. 20. Images of a snail shell taken with an MSGC operating with Xe-CH_4 at four bar [43].

[5] Defined as sparking rate divided by flux

B. TPC Readout

For the TESLA experiment at the future Linear Collider [40], a double or triple GEM configuration is under consideration [41,42] owing to its fast electron signal, minimal magnetic distortion effects, and suppression of ion feedback by design. Figure 21 shows some measurements and simulation of the fractional positive ion feedback in a double GEM [43].

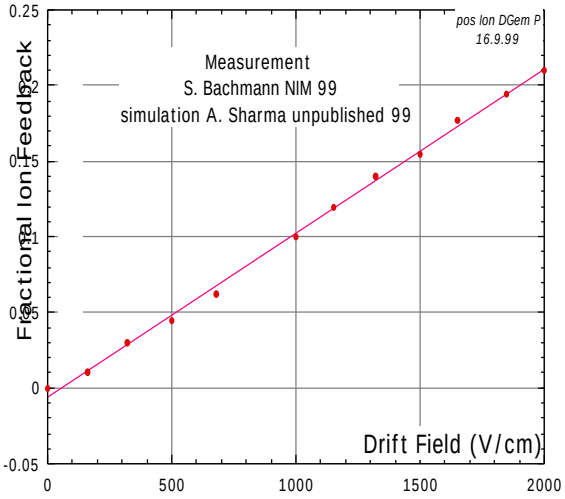

Fig. 21. Fractional ion feedback in the TPC drift volume (points are measurements [42], and a solid line is a computation).

Special hexagonal pads are being developed [41] proving unprecedented resolution of 50-60 μm in a TPC, using charge sharing and induction signals.

C. The MICROMEGAS X-ray Gallery

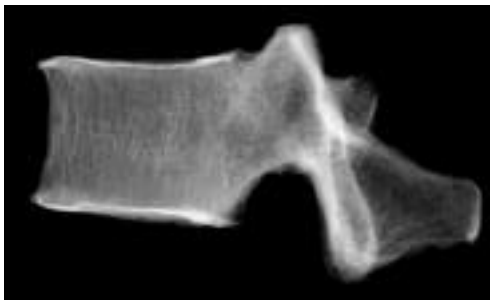

Fig. 22. The Radiographic image of a vertebra taken by MICROMEGAS.

Operating in pure Xenon at atmospheric pressure, the MICROMEGAS detectors have been developed for X-ray imaging. Figure 22 [45] shows an exampleof a vertebra scanned by MICROMEGAS.

D. Protein Crystallography SAXS (Small Angle X-Ray Scattering)

X-ray diffraction studies using MSGCs have yielded rapid analysis of single crystal structures by using the information of position and time of the incident X-rays: crystal structures of organic molecules can be obtained in a matter of minutes [46]. Fast time resolved X-ray diffraction measurements offer a time

variation of the SAXS pattern of a protein solution for example, shown in Fig. 23, within a frame time of 10 ms.

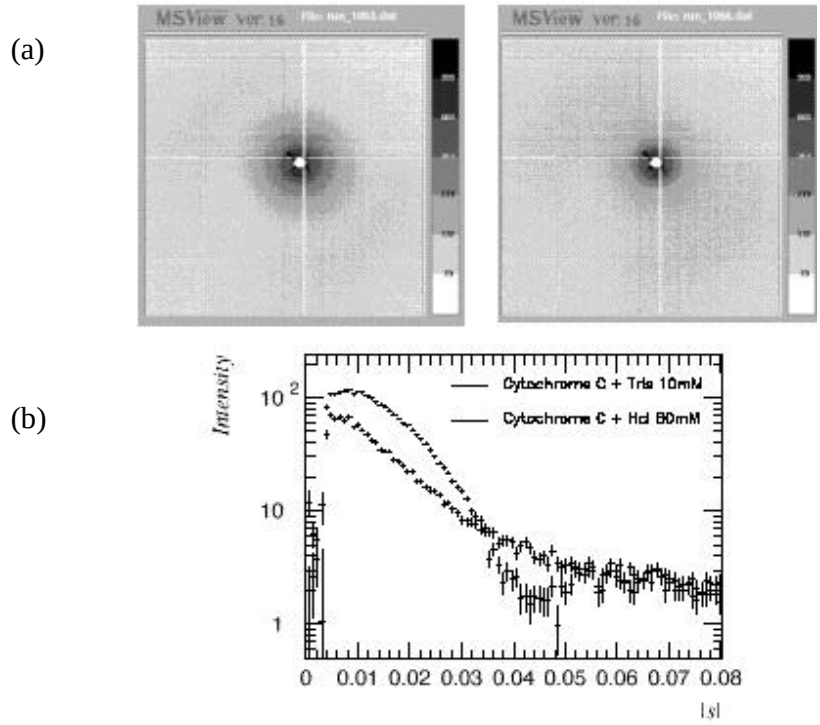

Fig. 23. (a) X-ray diffraction patterns of Cytochrome shows different concentrations of contamination molecules. (b) X-ray diffraction intensities of the same, measured more than a minute after mixing the solutions.

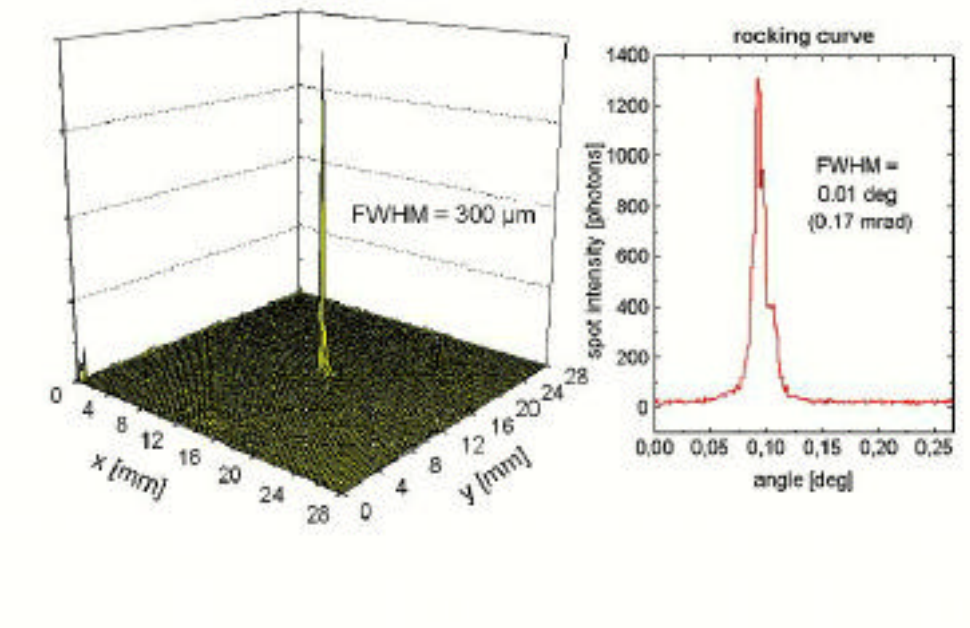

Fig. 24. A single intensive spot in the crystallogram of a protein crystal, collagen using VIP.

A diffraction pattern of a lipid membrane is shown in Fig. 24. The membrane was made with a VIP detector at Elettra (see section III.B above), a synchrotron source in Trieste, Italy. With complex algorithms, especially made for the readout cell border, and superimposing several shots of images, a high degree of detail may be obtained from diffraction patterns; see Fig. 25 and Ref. 26.

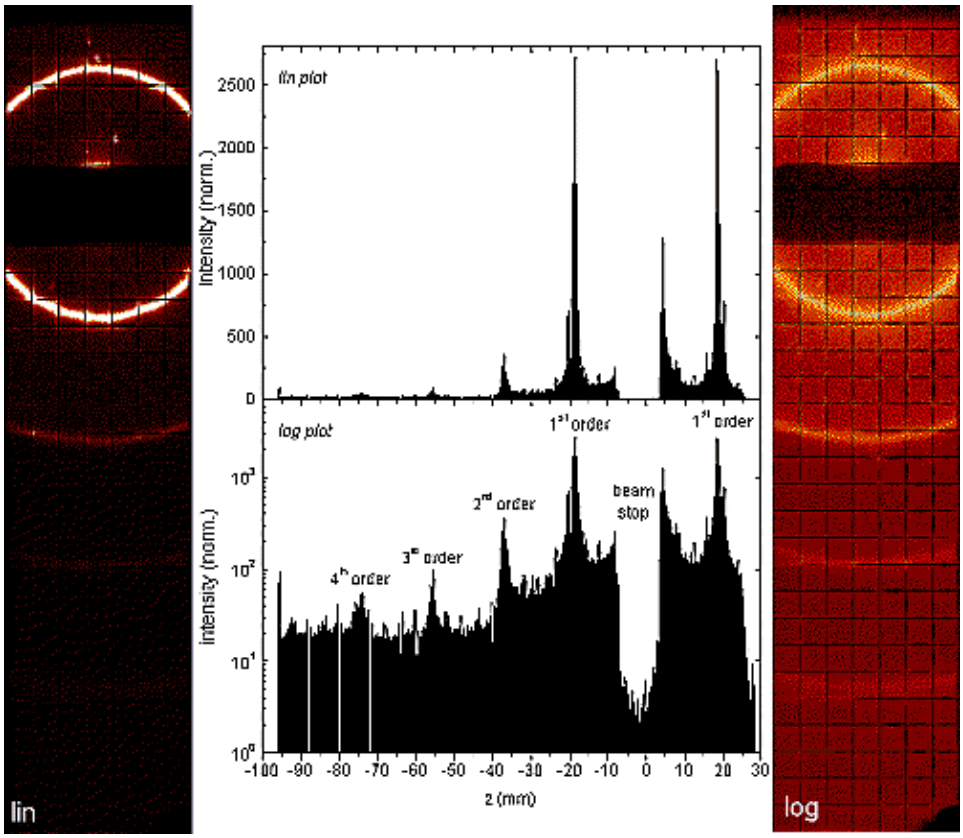

Fig. 25. Scan of the diffraction pattern of the lipid with a VIP; the middle part shows linear and logarithmic profiles of the pattern.

E. Digital Mammography UV and Visible Photomultipliers using GEM

The importance of early detection of cancer is obvious, small tumors are usually detected in routine radiographic scanning of the human body. Current radiographic equipment is limited in its detection capability by the limited contrast difference exhibited by malignant and benign tissues under given radiation doses. A combination of an x-ray converter, a MSGC, and a visible photocathode, shows great promise for a detector for digital mammography [47]. The essential features are a large flat area and high resolution. With a photocathode (UV, visible) coupled to a micropattern detector, the sealed gas avalanche photomultipliers are being developed for fast imaging of UV and visible light, as well as flat readout devices for scintillator and scintillating fiber arrays, and as medical imaging. Photocathodes have also been attempted by combining them with the Glass Capillary Plate (GCP) detectors [48], with the advantages of reduced photon-photon feedback and the high level of cleanliness necessary for the manufacture of high efficiency of photocathodes/secondary photon emitters.

To this end, single-photon detection has been actively pursued using a CsI photocathode coupled to three or four GEMs in tandem, and very large gains ~ 10^5 have been obtained in pure noble gas (Ar), and 10^6 with an admixture of few percent CH_4. [47]. With a small preamplification in the drift region, combined with high diffusion, fully efficient single-photon detection is predicted and measured [49,50] as demonstrated in figs. 26 (a and b). Fig. 27 shows an example of a large single-photon signal in Ar-CH_4 (95-5) with a three GEM combination [51].

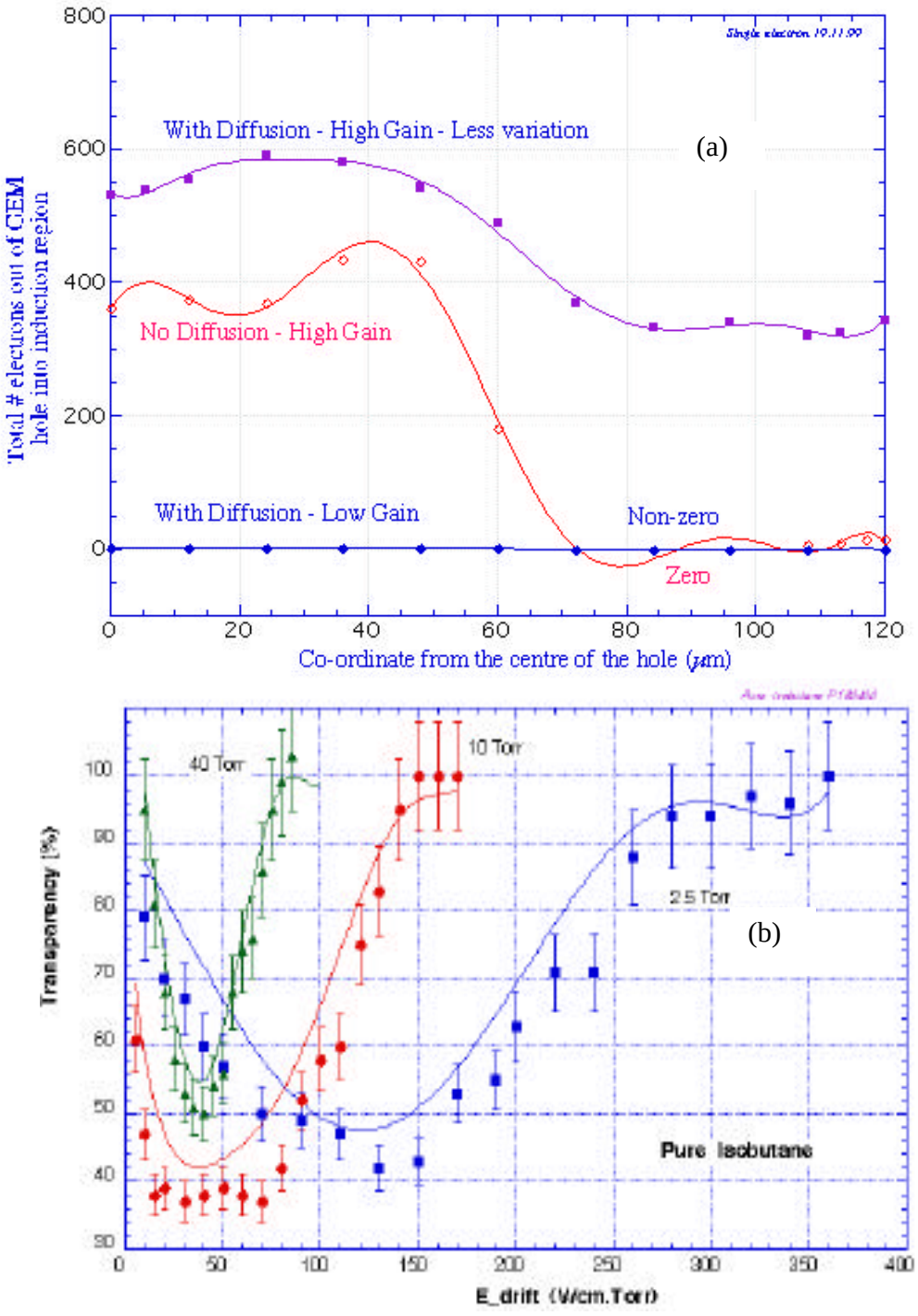

Fig. 26. (a) Transmission of single electrons amplified in a GEM, (b) Full efficiency of single electrons in a GEM with a transmissive photocathode and preamplification in the drift region.

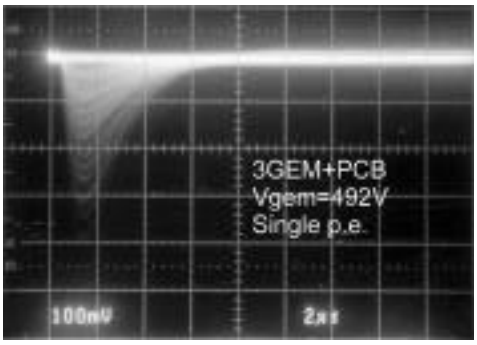

Fig. 27. Single-photon signals with a Triple GEM and CsI photocathode.

F. Cherenkov Ring Imaging (RICH/DIRC)

A feasibility study aimed at improving the detection of photons emitted by Cherenkov light, for example, for an upgrade of the existing SLD CRID at SLAC was made. Using a cascade of four GEMs and an operating gas as pure ethane, very high gains have been observed [49,52], as shown in Fig. 28.

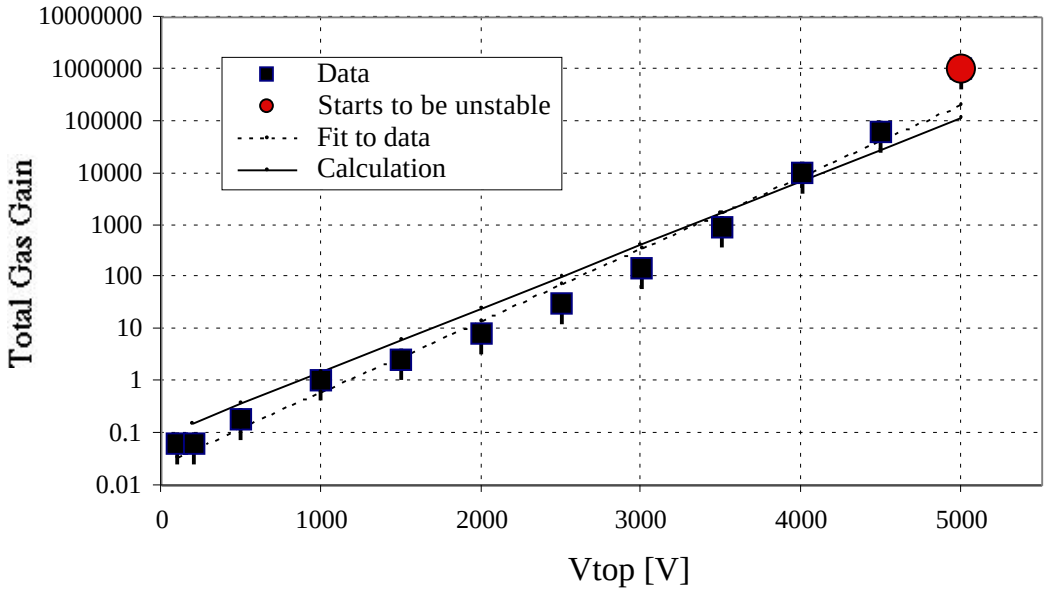

Fig. 28. Gain in a Quadruple GEM cascade in ethane gas at 1 bar and room temperature.

G. Scintillation Light Imaging

A novel application of micro-pattern technology was developed by integrating a MSGC in a gas proportional scintillation counter (GPSC) [53]. Instead of the usual photomultiplier tube, a reflective CsI photocathode was deposited on the microstrip plate surface of the MSGC that serves as the VUV photosensor for the scintillation light from xenon GPSC. This hybrid detector will be used to measure the Lamb shift in muonic hydrogen by detecting the 1.9-keV x-ray from the 2P-1S de-excitation, in a 5-T magnetic field [54].

With a GEM as amplifier and a CCD camera, images of individual projected alpha tracks are visible using the scintillation properties of Ar and CF_4, as shown in Fig. 29 [55]. The spectral distribution of the emitted light is analyzed in terms of the number of photons emitted per electron in the visible and near-infrared regions ($400<\lambda<1000$nm). The maximum number of photons emitted decreases with pressure.

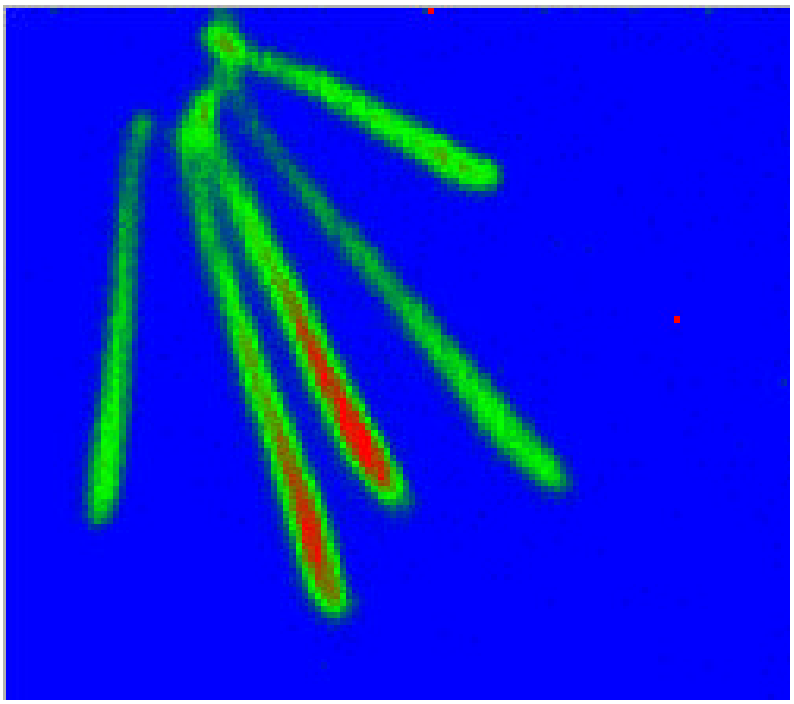

Fig. 29. Scintillation images of alpha tracks in Ar-CF_4.

H. X-ray imaging: Radiology and diagnostics

With a GEM + MSGC combination operating in Xe-CH_4 at 4 atm. X-ray images have been taken as an excellent example of imaging for diagnostics with a micro-pattern detector; see Fig. 30 and Ref. 41.

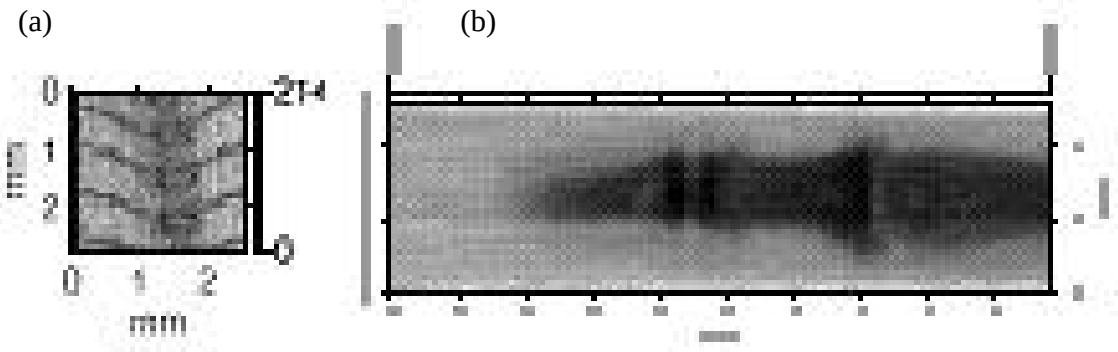

Fig. 30. (a) A 3 mm x 3 mm 13 kV X-ray absorption radiography of a fish bone taken at 2 atm. (b) a 3 mm x 10 mm 50 kV x-Ray digital image of a mouse.

Specialized two-dimensional readout boards have been manufactured using the GEM technology. Operating at ground potential, these boards, in conjunction with GEMs, have been developed for digital absorption radiography [43]. With a pixel size of 50 μm, the image of a mammal (small bat, width 32 mm) is shown in Fig. 31 taken from Ref. [42].

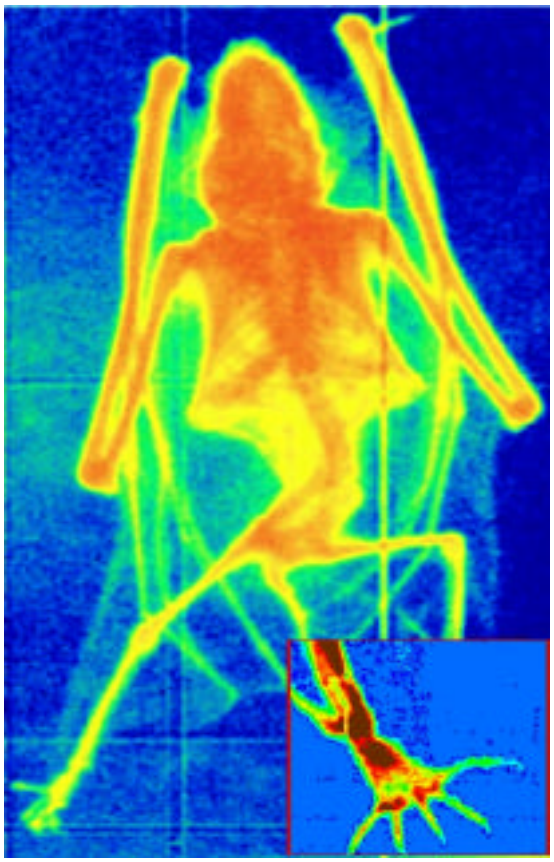

Fig. 31. Radiography of a small bat using GEM and 50μm x 50 μm 2D-readout.

I. Imaging of Polarized X-Rays

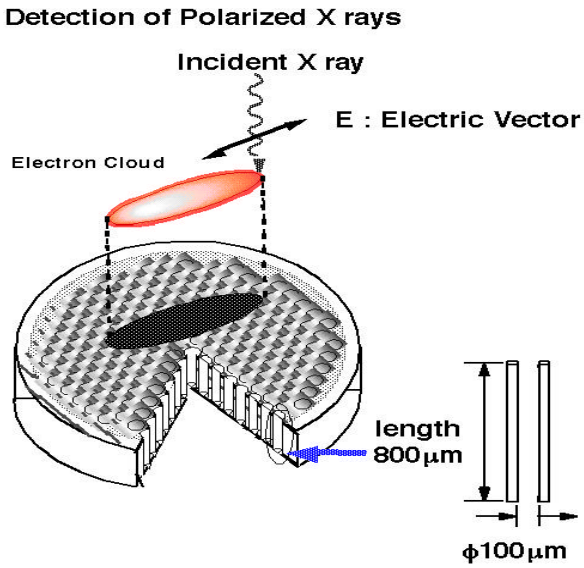

Fig. 32. Detection of polarized photons with a Glass Capillary Imaging Gas Proportional Counter.

In X-ray astronomy, measurements of X-ray polarization are useful to investigate features of magnetic fields such as pulsars, synchrotron nebulae, and so on. Some X-ray polarimeters have been developed using GCPs and GEMs [56-57] as exemplified in fig. 32. Because the emission direction of the primary electron depends on the polarization of the incident X-rays, the information on the polarization can be deduced, acquiring the information on the shape of electron clouds. The performance of the Polarimeter is expressed as the function of detection efficiency and modulation factor, and hence these parameters depend on gas pressure and gas depth. Figure 33 shows some images of tracks from a GCP [57].

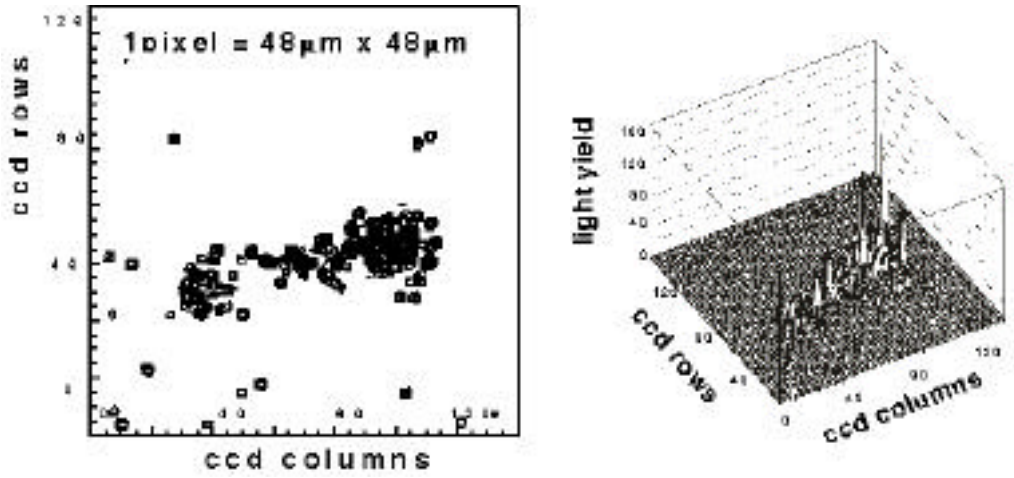

Fig. 33. Photoelectrons from a GCP Polarimeter.

J. GEM for Plasma Diagnostics

Exploiting the selective sensitivity and the high rate capability of GEM to soft X-rays, imaging the dynamics of fusion plasmas has been attempted by the Frascati and Pisa groups for the Frascati Tokamak Upgrade (FTU). With a GEM and individual pixel readout, time resolved plasma diagnostics are made giving information about temperature and turbulence effects. Figure 34 exemplifies the recognition of a steady state and collapsed plasma [58] by integrating counts over 50 μs in four adjacent channels.

(a)

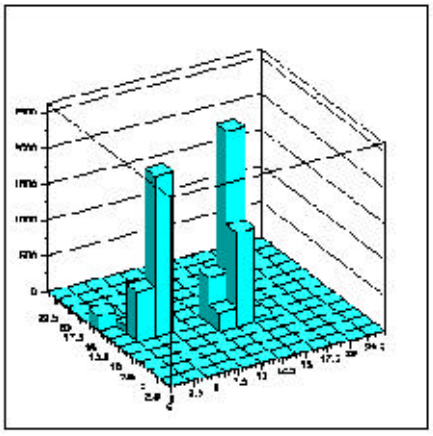

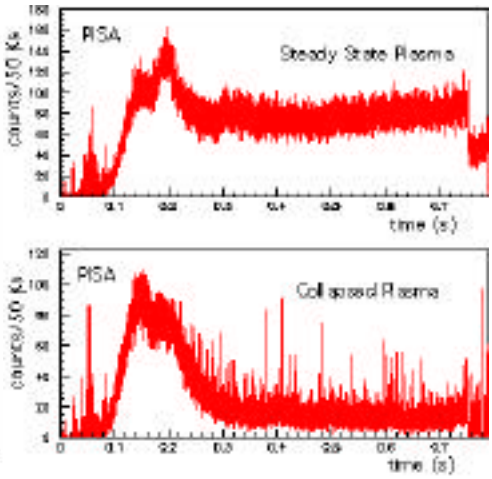

(b)

Fig. 34. (a) Reconstruction of photoelectrons with a GEM + micropixel readout, (b) Counts integrated in 50 μs for four adjacent pixels at the Frascati Toakamak [56].

V CONCLUSIONS AND OUTLOOK

Multiwire chambers have matured since their introduction over the last few decades, with several applications in particle physics and diagnostics of various kinds. The last decade has seen several novel developments in Micropattern Gaseous Detectors of which some have been summarized in this overview. Basic understanding of the discharge mechanisms in these devices has also improved, allowing amelioration of their design. Progress in the manufacture of customized readout boards has evolved, revolutionizing the potential applications of these detectors in radiology, diagnostics, astrophysics, and other fields.

VI REFERENCES

[1] Phil. Mag. Xiii(1896)392; Townsend and Raether, Conduction of electricity through gases (Ist ed, 1903); Proc. Of Royal Society, A81(1908)141

[2] G. Charpak et al Nucl. Instr. And Meth. 62(1968)262-268

[3] A. Breskin et al, Nucl. Instr. And Meth 161(1979)19; F. Sauli Physica Scripta 23(1981)526; G. Charpak and F. Sauli Ann. Rev. 34(1984)285, See also C. Grupen, Particle Detectors, Cambridge Press, 1996

[4] E. Babichev et al (1992) Nucl Instrum Methods Phys Res A323: 49, and references therein, S. Baru et al, Novosibirsk Preprint 35(1989) 98-39

[5] G. Kalifa et al, Pediatric. Radiology 28(1998)557

[6] E. Babichev et al in the Proceedings of Frontier Detectors for Frontier Physics Elba, Italy May 2000 & A. Porosev, in Proceeding of Frontier Detector for Frontier Physics, Elba May 2000.

[7] Martinez-Davalos et al, Evaluation of a new low-dose digital x-ray system. Phys Med Biol 38(1993)141

[8] Large Hadron Collider (LHC) at CERN

[9] A. Oed, Nucl. Instr. And Meth. A263(1988)35

[10] F. Sauli and A. Sharma, Annual Rev. of Nucl. Sci. 49(1999)41

[11] R. Bouclier et al Nuclear Physics B 61B (1998)315

[12] B. Boimska et al Nuclear Physics B 61B (1998) 498

[13] B. Schmidt , Nucl. Instr. And Meth. A419(1998)230

[14] V. Peskov et al, IEEE Transactions, Nucl. Sci. NS 45(1998)244

[15] A. Bressan et al Nucl. Instr. And Meth. A 424(1998)321

[16] P. Fonte et al Nucl. Instr. And Meth. A 419(1998) 405

[17] J. Kadyk et al Nuclear Physics B 61B (1998) 258

[18] C. A. Spindt et al., The Micro-needle Concept, J. Appl. Phys. 47(1976)5248; both experimental attempts of Va'vra and Oed were unpublished; see J. Va'vra, SSC Proposal 81187, 1987.

[19] S.F. Biagi et al, Nucl. Instrum. Methods A371(1995)12

[20] A. Bressan, A. Buzulutskov, L. Ropelewski, F.Sauli and L. Shekhtman, Nucl. Instr. And Meth. A 432(1999)119-124

[21] Y. Giomataris et al Nucl. Instr. And Meth. A 376(1996)29

[22] A. Sharma, ICFA Bulletin Fall 1999 http://www.slac.stanford.edu/pubs/icfa

[23] F. Kuune in Proceeding of Frontier Detector for Frontier Physics, Elba May 2000

[24] F. Bartol et al., J. Phys. III France 6 (1996)337, G. Chaplier et al Nucl. Instr. And Meth A426(1999)

[25] A. Sarvestani et al Nucl. Instr. And Meth. A 419(1998)444

[26] N. Pavel, Siegen, Priv. Com. Oct 2000

[27] F. Sauli Nucl. Instr. And Meth. A 386(1997)531

[28] B. Adeva et al., Nucl. Instr. And Meth A 419(1998)405

[29] P. Rehak et al Proceedings IEEE Nuclear Science Symposium 1999, Seattle USA

[30] W. K. Pitts et al Nucl. Instr. And Meth A438(1999)277

[31] W. K. Pitts See also Proceedings, IEEE Nuclear Science Symposium 1999, Seattle USA

[32] R. Bellazzini et al, Nucl. Instr. And Meth. A 423(1998)125

[33] R. Bellazzini et al, Nucl. Instr. And Meth. A 424(1998)444

[34] C. Richter, PhD. Thesis October 2000 submitted to University of Heidelberg, Germany.

[35] F. Gomez Private Communication and Internal Notes. T. Nunez, and P. Vasquez Theses 1999, Santiago University, Spain.

[36] J. Benlloch et al, IEEE trans NUCl. Sci. NS-45(1998) 234, J. Benlloch et al NIMA 419 (1998) 410
[37] B. Ketzer, Contribution to this Conference
[38] M. Ziegler et al hep-ex/0007007/July 2000, LHC-B Internal Tracking Notes: 99-024, 2000-013, 2000-15, 2000-056, U. Straumann Proceedings, Imaging 2000, Stockholm.
[39] M. Dixit et al, IEEE Trans. 47(1998)809; D. G. Gobbi et al, Phys. Med. Biol. 44(1999)1317
[40] The future TESLA Linear Collider at DESY Hamburg, DESY 97/048
[41] M. Dixit in Proceedings of Imaging 2000, Stockholm.
[42] A.Bressan et al Nucl. Instr. And Meth. A 425(1999)254, 262
[43] A. Bressan et al Nucl. Instr. And Meth. A 423(1999)424
[44] A. Sharma, Nucl. Instr. and Meth. A454(2000)267 Proceedings of Symposium on Applications of Particle Detectors in Medicine, Biology and Astrophysics, 5-8 October 1999, Siegen, Germany, also printed as CERN-OPEN-99/373.
[45] G. Charpak and M. Meynadier Priv. Com. Oct. 2000
[46] S. Ochi et al, SPIE Proceedings 5(1998)324
[46] DIGITAL MAMMOGRAPHY Project MICADO within Weizman, Pisa, Brussels, and Agfa Gaevert.
[47] A. Breskin et al NIM A 442(2000)58
[48] V. Peskov et al NIM A433(1999)492,V. Peskov etal IEEE Trans. Nucl. Science NS-45(1999)244, and contribution to this conference.
[49] A. Sharma CERN Preprint 99/372, Submitted for publication to Nucl. Instr. & Meth. (1999), See also Proceedings of Imaging 2000, Stockholm, June 2000.
[50] C. Richter et al To Appear in the Proceedings of Frontier Detectors for Frontier Physics, Elba 2000. Submitted Nucl. Instr. And Meth.
[51] A.Buzulutskov et al. Nucl. Intr. And Meth A443(2000)164-180, A 433(1999)471, andContribution to Nuclear Science Symposium and Medical Imaging conference, Oct 2000
[52] J. Va'vra Priv. Com. April 2000, and [49]
[53] J.F.C.A. Veloso et al Nucl. Instr. And Meth. A In Press
[54] J.F.C.A.Veloso et al Nuc. Instr. And Meth A In Press
[55] F. Fraga et al, in Nuclear Science Symposium and Medical Imaging conference, Oct 2000, Lyon
[56] H. Sakurai et al. "A new type of proportional counter using a capillary plate" NIM A374(1996)341-344,
[57] T.Masuda et al. IEEE Trans NS 47, 2000.
[58] R. Bellazzini et al, Proceedings of Imaging 2000, Stockholm.